

1 Local forest structure variability increases resilience to wildfire in 2 dry western U.S. coniferous forests

3 Michael J. Koontz^{1,2,3*}, Malcolm P. North^{2,4}, Chhaya M. Werner^{2,5,6}, Stephen E. Fick^{7,8}, Andrew M. Latimer²

4 ¹Graduate Group in Ecology, University of California; Davis, CA, USA

5 ²Department of Plant Sciences, University of California; Davis, CA, USA

6 ³Earth Lab, University of Colorado-Boulder; Boulder, CO, USA

7 ⁴Pacific Southwest Research Station, USDA Forest Service; Mammoth Lakes, CA, USA

8 ⁵Center for Population Biology, University of California; Davis, CA, USA

9 ⁶German Centre for Integrative Biodiversity Research; Halle-Jena-Leipzig, Germany

10 ⁷US Geological Survey, Southwest Biological Science Center

11 ⁸Department of Ecology and Evolutionary Biology, University of Colorado; Boulder, CO, USA

12 *Correspondence: 4001 Discovery Drive; Boulder, CO 80303; michael.koontz@colorado.edu

13 Coauthor emails: mnorth@ucdavis.edu (MPN), cwerner@ucdavis.edu (CMW), stephen.fick@gmail.com (SEF),
14 amlatimer@ucdavis.edu (AML)

15 *Running title:* Remote sensing resilience

16 *Keywords:* resilience, wildfire, severity, texture analysis, forest structure, Sierra Nevada, forest, disturbance

17 *Type of article:* Letters

18 *Abstract word count:* 149

19 *Main text word count:* 4805 (Intro: 930; Methods: 1631; Results: 558; Discussion: 1686)

20 *Text boxes word count:* 0

21 *Number of...* references: 106, figures: 5, tables: 1, text boxes: 0

22 *Statement of authorship:* MJK, CMW, SEF, MPN, and AML conceived the study. MJK, SEF, and CMW
23 wrote the Earth Engine code. MJK performed the analysis, with input from all authors. MJK wrote the first
24 draft of the manuscript. All authors contributed substantially to editing and revisions.

25 *Data accessibility statement:* Data and analysis code are available on the Open Science Framework at
26 <https://osf.io/27nsr/>.

27 *Date report generated:* July 22, 2019

28 **Abstract**

29 A “resilient” forest endures disturbance and is likely to persist. Resilience to wildfire may arise from feedback
30 between fire behavior and forest structure in dry forest systems. Frequent fire creates fine-scale variability
31 in forest structure, which may then interrupt fuel continuity and prevent future fires from killing overstory
32 trees. Testing the generality and scale of this phenomenon is challenging for vast, long-lived forest ecosystems.
33 We quantify forest structural variability and fire severity across >30 years and nearly 1,000 wildfires in
34 California’s Sierra Nevada. We find that greater variability in forest structure increases resilience by reducing
35 rates of fire-induced tree mortality and that the scale of this effect is local, manifesting at the smallest spatial
36 extent of forest structure tested (90m x 90m). Resilience of these forests is likely compromised by structural
37 homogenization from a century of fire suppression, but could be restored with management that increases
38 forest structural variability.

39 **Introduction**

40 Forests are essential components of the biosphere, and ensuring their persistence is of high management
41 priority given their large carbon stores and other valued ecosystem services (1–4). Modern forests are
42 subject to disturbances that are increasingly frequent, intense, and entangled with human society, which may
43 compromise their resilience and their ability to persist (3, 5, 6). A resilient forest can absorb disturbances
44 and may reorganize, but is unlikely to transition to an alternate vegetation type in the long run (7–10).
45 Resilience can arise when interactions amongst heterogeneous elements within a system create stabilizing
46 negative feedbacks, or interrupt positive feedbacks that would otherwise cause critical transitions (10, 11).
47 System resilience can be generated by heterogeneity at a variety of organizational scales, including genetic
48 diversity (12–14), species diversity (15–17), functional diversity (18), topoclimatic complexity (19, 20), and
49 temporal environmental variation (21). Forest resilience mechanisms are fundamentally difficult to quantify
50 because forests comprise long-lived species, span large geographic extents, and are affected by disturbances at
51 a broad range of spatial scales (10, 22). It is therefore critical, but challenging, to understand the system-wide
52 mechanisms underlying forest resilience and the extent to which humans have the capacity to influence them.
53 Wildfire severity describes a fire’s effect on vegetation (23) and high-severity fire, in which all or nearly all
54 overstory vegetation is killed, can be a precursor to state transitions in dry coniferous forests (24, 25). For
55 several centuries prior to Euroamerican invasion, fire regimes in this ecosystem were variable, having primarily
56 low- and moderate-severity fire, but localized patches of high-severity fire (26). Most dry coniferous tree
57 species in frequent-fire forests did not evolve mechanisms to protect propagules (e.g., seeds, buds/stems that

58 can resprout) through high-severity fire, so recruitment in large patches with few or no surviving trees is
59 often highly limited by longer-distance dispersal of tree seeds from unburned or lower-severity areas (24, 27,
60 28). Absence of tree seeds after severe wildfire can lead to forest regeneration failure as resprouting shrubs
61 outcompete slower-growing conifer seedlings and provide continuous cover of flammable fuel that makes future
62 high-severity wildfire more likely (29, 30). Dry forest regeneration is especially imperiled after high-severity
63 fire when post-fire climate conditions are suboptimal for conifer seedling establishment (25) or optimal for
64 shrub regeneration (28).

65 Many dry western U.S. forests are experiencing “unhealthy” conditions which leaves them prone to catastrophic
66 shifts in ecosystem type (3). First, warmer temperatures coupled with recurrent drought (i.e., “hotter
67 droughts”) exacerbate water stress on trees (3, 31, 32), producing conditions favorable for high-intensity fire
68 (33, 34) and less suitable for post-fire conifer establishment (25, 35). Second, a century of fire suppression
69 has drastically increased forest density and fuel connectivity (26), which favors modern wildfires with large,
70 contiguous patches of tree mortality whose interiors are far from potential seed sources (24, 26, 36, 37). Thus,
71 the presence of stabilizing feedbacks that limit high-severity fire may represent a fundamental resilience
72 mechanism of dry coniferous forests, but anthropogenic climate and management impacts may be upsetting
73 those feedbacks and eroding forest resilience.

74 An emerging paradigm in forest ecology is that resilience to disturbances such as wildfire may derive from
75 heterogeneity in vegetation structure (38–40). Forest structure– the size and spatial distribution of vegetation
76 in a forest– links past and future fire disturbance via feedbacks with fire behavior (41). A structurally
77 variable forest with horizontally and vertically discontinuous fuel may experience slower-moving surface fires,
78 a lower probability of crown fire initiation and spread, and a reduced potential for self-propagating, eruptive
79 behavior (11, 42–45). Feeding back to influence forest structure, this milder fire behavior, characteristic of
80 pre-Euroamerican settlement conditions in dry western U.S. forests, generates a heterogeneous patchwork of
81 fire effects including consumed understory vegetation, occasional overstory tree mortality, and highly variable
82 structure at a fine scale (26, 46, 47). Thus, more structurally variable dry forests are often considered more
83 resilient and are predicted to persist in the face of frequent wildfire disturbance (38, 43, 48).

84 While the homogenizing effect of modern high-severity fire on forest structure is well-documented (37), the
85 foundational concept of feedback between heterogeneity of forest structure and fire severity is underexplored, in
86 part because of the challenge of measuring fine-scale heterogeneity at broad spatial extents (49). Furthermore,
87 it has been difficult to empirically resolve the “scale of effect” (49) for how variability in forest structure is
88 meaningful for resilience (50, 51).

89 Recent advances in the accessibility and tractability of spatiotemporally extensive Earth observation data
90 (52) provide an avenue to insight into fundamental ecosystem properties at relevant scales, such as resilience
91 mechanisms of vast, long-lived forests. We use Landsat satellite imagery and leverage a massively-parallel
92 image processing approach to calculate wildfire severity for nearly 1,000 Sierra Nevada yellow pine/mixed-
93 conifer wildfires encompassing a wide size range (4 to >100,000 hectares) and long time series (1984 to 2017).
94 We calibrate these spectral severity measures to ground assessments of fire effects on overstory trees from
95 over 200 field plots. For each point within these ~1,000 fires, we use texture analysis (53) at multiple scales
96 in order to characterize local variability in vegetation structure across broad spatial extents and determine its
97 “scale of effect” (49). We pair the resulting extensive database of wildfire severity and multiple scales of local
98 forest variability to ask: (1) Does spatial variability in forest structure increase the resilience of California
99 yellow pine/mixed-conifer forests by reducing the severity of wildfires? (2) What is the “scale of effect” of
100 structural variability that influences wildfire severity? and (3) Does the influence of structural variability on
101 fire severity depend on topography, regional climate, or other conditions?

102 **Material and Methods**

103 **Study system**

104 Our study assesses the effect of vegetation structure on wildfire severity in the Sierra Nevada mountain
105 range of California in yellow pine/mixed-conifer forests (Fig. 1). This system is dominated by a mixture of
106 conifer species including ponderosa pine (*Pinus ponderosa*), sugar pine (*Pinus lambertiana*), incense-cedar
107 (*Calocedrus decurrens*), Douglas-fir (*Pseudotsuga menziesii*), white fir (*Abies concolor*), and red fir (*Abies*
108 *magnifica*), angiosperm trees primarily including black oak (*Quercus kelloggii*), as well as shrubs (*Ceanothus*
109 spp., *Arctostaphylos* spp.) (26). We considered “yellow pine/mixed-conifer forest” to be all areas designated
110 as a yellow pine, dry mixed-conifer, or moist mixed-conifer pre-settlement fire regime (PFR) in the USFS
111 Fire Return Interval Departure database ([https://www.fs.usda.gov/detail/r5/landmanagement/gis/?cid=](https://www.fs.usda.gov/detail/r5/landmanagement/gis/?cid=STELPRDB5327836)
112 [STELPRDB5327836](https://www.fs.usda.gov/detail/r5/landmanagement/gis/?cid=STELPRDB5327836)), which reflects potential vegetation and is less sensitive to recent land cover change
113 (37). We considered the Sierra Nevada region to be the area within the Sierra Nevada Foothills, the High
114 Sierra Nevada, and the Tehachapi Mountain Area Jepson ecoregions (54).

115 **A programmatic remote sensing assessment of wildfire severity**

116 We measured forest vegetation characteristics and wildfire severity using imagery from the Landsat series
117 of satellites (36, 55) post-processed to surface reflectance using radiometric corrections (56–59). Landsat

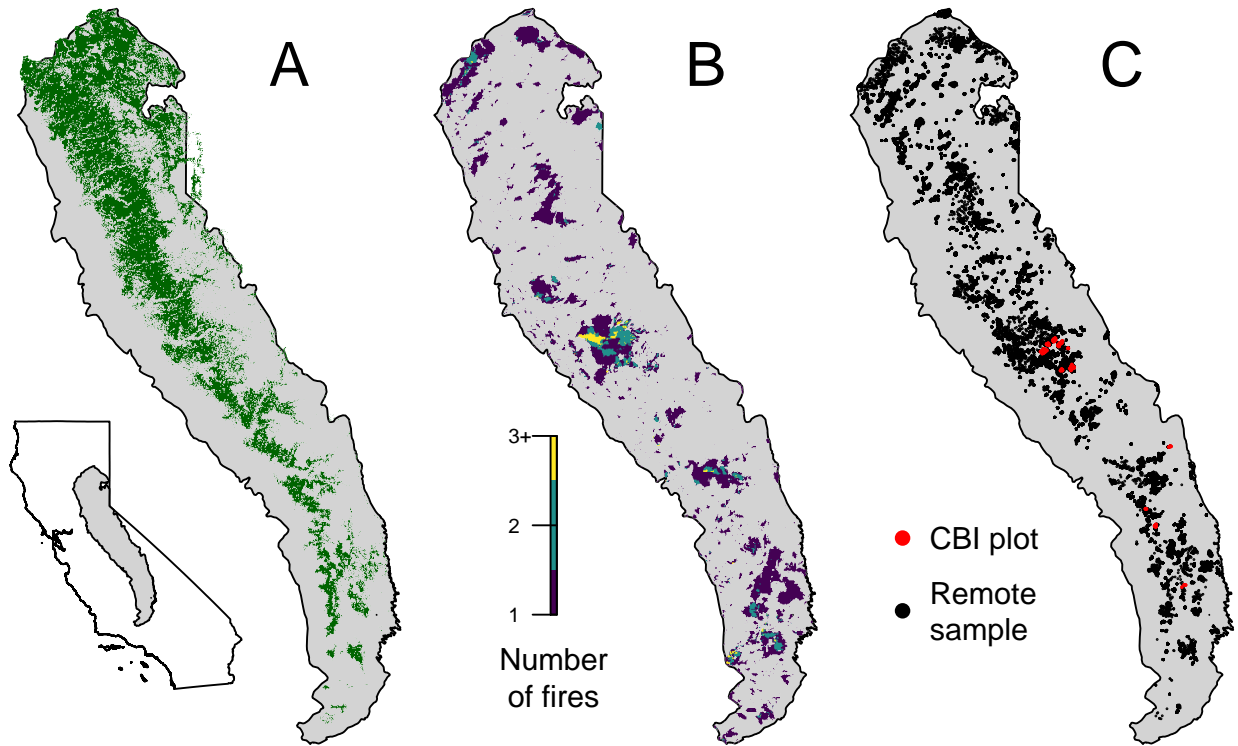


Fig. 1. Geographic setting of the study. A) Location of yellow pine/mixed-conifer forests as designated by the Fire Return Interval Departure (FRID) product which, among other things, describes the potential vegetation in an area based on the pre-Euroamerican settlement fire regime. B) Locations of all fires covering greater than 4 hectares that burned in yellow pine/mixed-conifer forest between 1984 and 2017 in the Sierra Nevada mountain range of California according to the State of California Fire Resource and Assessment Program database, the most comprehensive database of fire perimeters of its kind. Colors indicate how many fire perimeters overlapped a given pixel within the study time period. C) (red) Locations of 208 composite burn index (CBI) ground plots used to calibrate the remotely sensed measures of severity. (black) Locations of random samples drawn from 972 unique fires depicted in panel B that were in yellow pine/mixed-conifer forest as depicted in panel A, and which were designated as “burned” by exceeding a threshold relative burn ratio (RBR) determined by calibrating the algorithm presented in this study with ground-based CBI measurements.

118 satellites image the entire Earth approximately every 16 days with a 30m pixel resolution. We used Google
119 Earth Engine, a massively parallel cloud-based geographic information system and image hosting platform,
120 for all image collation and processing (52).

121 We calculated wildfire severity for the most comprehensive digital record of fire perimeters in California: The
122 California Department of Forestry and Fire Protection, Fire and Resource Assessment Program (FRAP) fire
123 perimeter database (http://frap.fire.ca.gov/projects/fire_data/fire_perimeters_index). Smaller fire events
124 are important contributors to fire regimes, but their effects are often underrepresented in analyses of fire
125 effects (60). The FRAP database includes all known fires that covered more than 4 hectares, compared to
126 the regional standard database which includes fires covering greater than 80 hectares (36, 37, 61, 62) and the
127 national standard Monitoring Trends in Burn Severity (MTBS) database which includes fires covering greater
128 than 400 hectares in the western U.S. (55). Using the FRAP database of fire perimeters, we quantified fire
129 severity within each perimeter of 972 wildfires in the Sierra Nevada yellow pine/mixed-conifer forest that
130 burned between 1984 and 2017, which more than doubles the number of fire events represented from 430 to
131 972 compared to the regional standard database.

132 We created per-pixel median composites of collections of pre- and postfire images for each fire to calculate
133 common spectral indices of wildfire severity. Prefire image collections spanned a fixed time window ending
134 one day before the fire’s discovery date and postfire image collections spanned the same fixed time window,
135 exactly one year after the prefire window. We tested four different time periods (16, 32, 48, and 64 days) that
136 defined the time window of the pre- and postfire image collections, and seven common spectral indices of
137 severity (RBR, dNBR, RdNBR, dNBR2, RdNBR2, dNDVI, RdNDVI) for a total of 28 different means to
138 remotely measure wildfire severity. See supplemental methods for full details of spectral measures of wildfire
139 severity.

140 We calibrated these 28 severity metrics with 208 field measures of fire effects to overstory vegetation—the
141 overstory component of the Composite Burn Index (CBI)—from two previously published studies (63, 64).
142 CBI is a metric of vegetation mortality across several vertical vegetation strata within a 30m diameter field
143 plot, and the overstory component characterizes fire effects to the overstory vegetation specifically (65). CBI
144 ranges from 0 (no fire impacts) to 3 (very high fire impacts), and has a long and successful history of use as a
145 standard for calibrating remotely-sensed severity data in western U.S. forests (36, 65–70). We interpolated
146 each remotely-sensed severity metric using both bilinear (mean of 4 nearest pixels) and bicubic interpolation
147 (mean of 16 nearest pixels) (67, 68, 70) and fit a non-linear model following (36), (66), (68), and (70) to each
148 remotely-sensed severity metric of the following form:

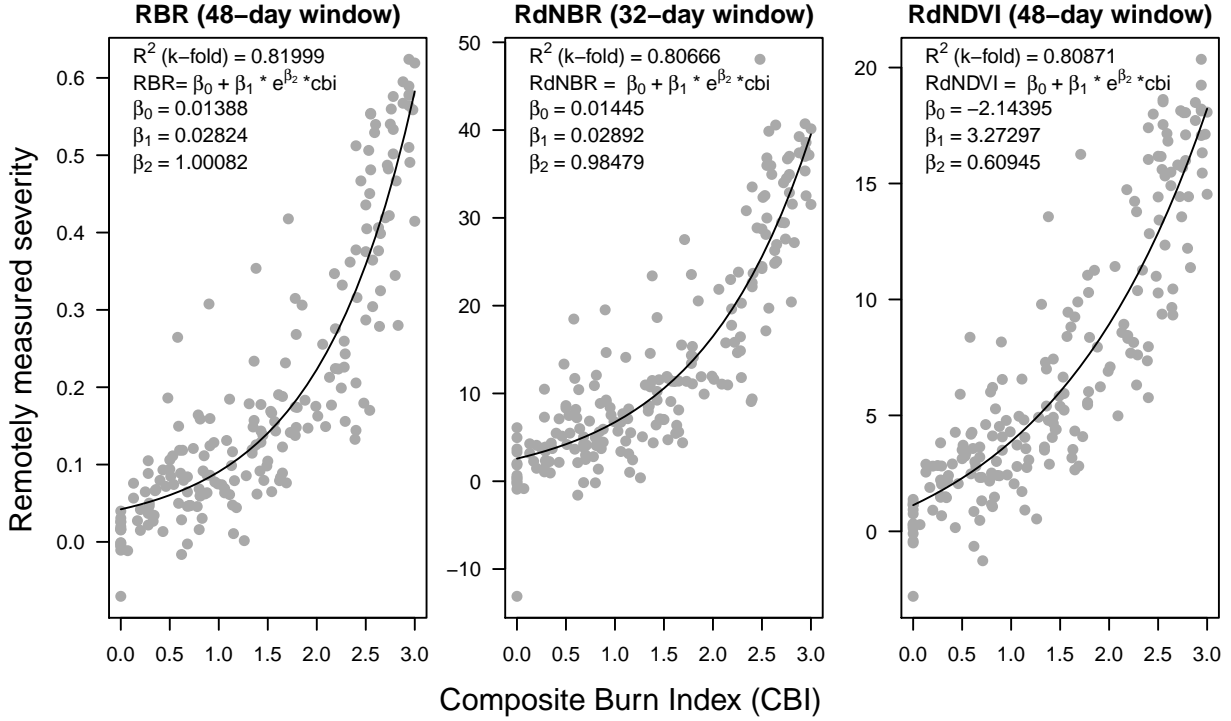


Fig. 2. Three top performing remotely-sensed severity metrics based on 5-fold cross validation (relative burn ratio, 48-day window, bicubic interpolation; relative delta normalized burn ratio, 32-day window, bilinear interpolation; and relative delta normalized difference vegetation index, 48-day window, bilinear interpolation) calculated using new automated image collation algorithms, calibrated to 208 field measures of fire severity (composite burn index). See Supplemental Table 1 for performance of all tested models.

149 (1) $remote_severity = \beta_0 + \beta_1 e^{\beta_2 cbi_overstory}$

150 We performed five-fold cross validation using the `modelr` and `purrr` packages in R (71–73). To compare
 151 goodness of model fits with (36), (66), and (68), we report the average R^2 value from the cross validation for
 152 each of the models. We used the severity calculation derived from the best fitting model from this comparison
 153 for all further analyses, which used a 48-day time window and the Relative Burn Ratio (RBR; (68)) spectral
 154 index (5-fold cross validation $R^2 = 0.82$; first panel of Fig. 2; Supp. Table 1). Example algorithm outputs
 155 are shown in Fig. 3.

156 Using the non-linear relationship between RBR and CBI from the best performing calibration model, we
 157 calculated the threshold RBR corresponding to “high-severity” signifying complete or near-complete overstory
 158 mortality using the common CBI high-severity lower threshold of 2.25 (i.e., an RBR value of 0.282) (36).

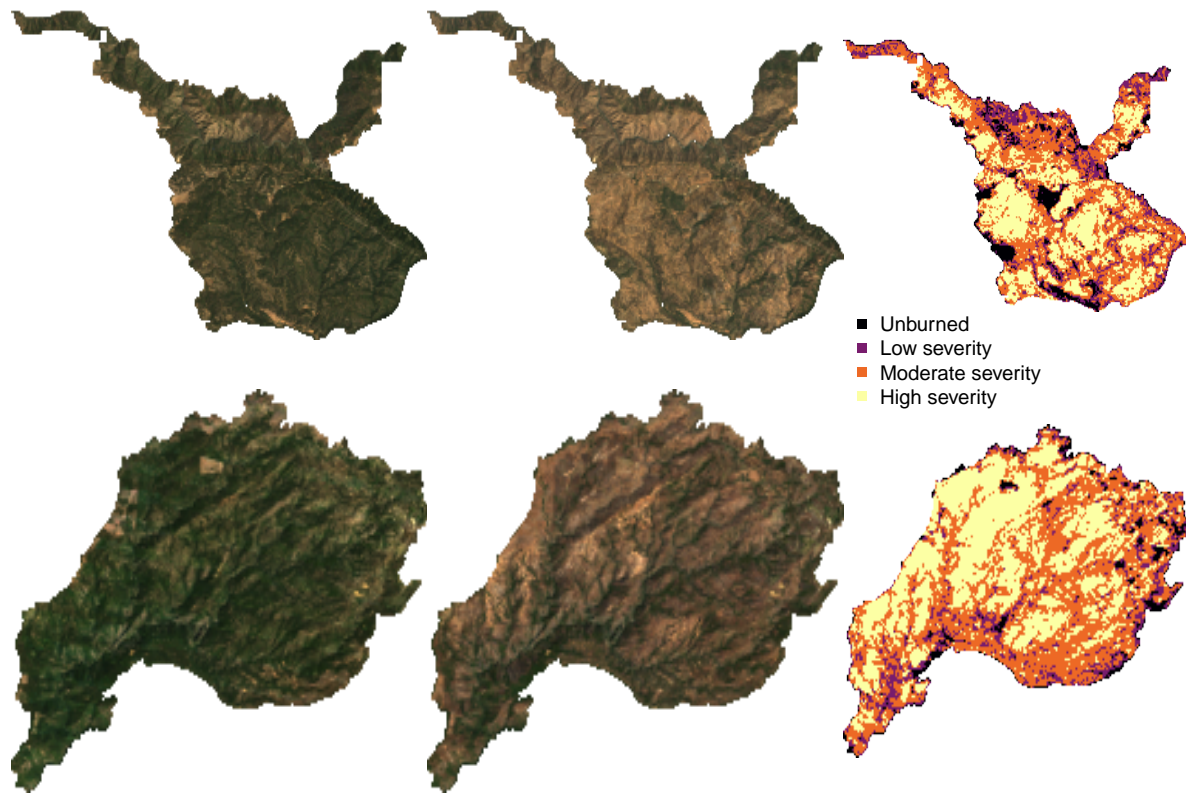


Fig. 3. Example algorithm outputs for the Hamm Fire of 1987 (top half) and the American Fire of 2013 (bottom half) showing: prefire true color image (left third), postfire true color image (center third), relative burn ratio (RBR) calculation using a 48-day image collation window before the fire and one year later (right third). For visualization purposes, these algorithm outputs have been resampled to a resolution of 100m x 100m from their original resolution of 30m x 30m. Data used for analyses were sampled from the outputs at the original resolution.

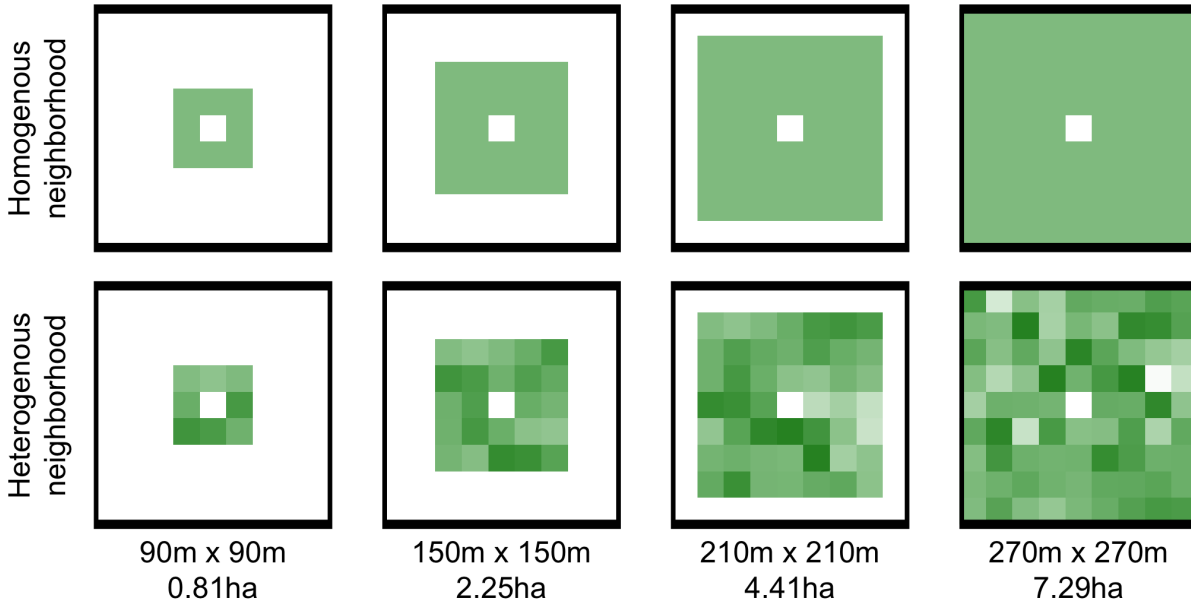


Fig. 4. Example of homogenous forest (top row) and heterogenous forest (bottom row) with the same mean NDVI values (~ 0.6). Each column represents forest structural variability measured using a different neighborhood size.

159 Remotely sensing local variability in forest structure at broad extents

160 We used texture analysis to calculate a remotely-sensed measure of local forest variability (53, 74). Within a
 161 moving square neighborhood window with sides of 90m (3x3 pixels), 150m (5x5 pixels), 210m (7x7 pixels),
 162 and 270m (9x9 pixels), we calculated forest variability for each pixel as the standard deviation of the NDVI
 163 values of its neighbors (not including itself). NDVI correlates well with foliar biomass, leaf area index, and
 164 vegetation cover (75), so a higher standard deviation of NDVI within a given local neighborhood corresponds
 165 to discontinuous canopy cover and abrupt vegetation edges (see Fig. 4) (76). Canopy cover is positively
 166 correlated with surface fuel loads including dead and down wood, grasses, and short shrubs (77, 78), which
 167 are primarily responsible for initiation and spread of “crowning” fire behavior which kills overstory trees (79).

168 Remote sensing other conditions

169 Topographic conditions

170 Elevation data were sourced from the Shuttle Radar Topography Mission (80), a 1-arc second digital elevation
 171 model. Slope and aspect were extracted from the digital elevation model. Per-pixel topographic roughness
 172 was calculated as the standard deviation of elevation values within the same-sized kernels as those used for
 173 variability in forest structure (90m, 150m, 210m, and 270m on a side and not including the central pixel).

174 We used the digital elevation model to calculate the potential annual heat load at each pixel, which is an
175 integrated measure of latitude, slope, and a folding transformation of aspect about the northeast-southwest
176 line ((81) with correction in (82); See Supplemental Methods for equations)

177 **Moisture conditions**

178 The modeled 100-hour fuel moisture data were sourced from the gridMET product, a gridded meteorological
179 product with a daily temporal resolution and a 4km x 4km spatial resolution (83). We calculated 100-hour
180 fuel moisture as the median 100-hour fuel moisture for the 3 days prior to the fire. The 100-hour fuel moisture
181 is a correlate of the regional temperature and moisture which integrates the relative humidity, the length of
182 day, and the amount of precipitation in the previous 24 hours. Thus, this measure is sensitive to multiple
183 hot dry days across the 4km x 4km spatial extent of each grid cell, but not to diurnal variation in relative
184 humidity nor to extreme weather events during a fire.

185 **Remote samples**

186 Approximately 100 random points were selected within each FRAP fire perimeter in areas designated as
187 yellow pine/mixed-conifer forest and the values of wildfire severity as well as the values of each covariate were
188 extracted at those points using nearest neighbor interpolation. Using the calibration equation described in
189 Eq. 1 for the best configuration of the remote severity metric, we removed sampled points corresponding to
190 “unburned” area prior to analysis (i.e., below an RBR threshold of 0.045). The random sampling amounted
191 to 54109 total samples across 972 fires.

192 **Modeling the effect of forest variability on severity**

193 We used a hierarchical logistic regression model (Eq. 2) to assess the probability of high-severity wildfire as a
194 linear combination of the remote metrics described above: prefire NDVI of each pixel, standard deviation of
195 NDVI within a neighborhood (i.e., forest structural variability), the mean NDVI within a neighborhood, 100-
196 hour fuel moisture, potential annual heat load, and topographic roughness. We included two-way interactions
197 between the structural variability measure and prefire NDVI, neighborhood mean NDVI, and 100-hour fuel
198 moisture. We include the two-way interaction between a pixel’s prefire NDVI and its neighborhood mean
199 NDVI to account for structural variability that may arise from contrasts between these variables (e.g., “holes
200 in the forest” vs. “isolated patches”; see Supplemental Fig. 2). We scaled all predictor variables, used
201 weakly-regularizing priors, and estimated an intercept for each individual fire with pooled variance.

$$severity_{i,j} \sim \text{Bern}(\phi_{i,j})$$

$$\beta_0 +$$

$$\beta_{\text{nbhd_stdev_NDVI}} * \text{nbhd_stdev_NDVI}_i +$$

$$\beta_{\text{prefire_NDVI}} * \text{prefire_NDVI}_i +$$

$$\beta_{\text{nbhd_mean_NDVI}} * \text{nbhd_mean_NDVI}_i +$$

$$\beta_{\text{fm100}} * \text{fm100}_i +$$

$$202 \quad (2) \quad \text{logit}(\phi_{i,j}) = \beta_{\text{pahl}} * \text{pahl}_i +$$

$$\beta_{\text{topographic_roughness}} * \text{topographic_roughness}_i +$$

$$\beta_{\text{nbhd_stdev_NDVI} * \text{fm100}} * \text{nbhd_stdev_NDVI}_i * \text{fm100}_i +$$

$$\beta_{\text{nbhd_stdev_NDVI} * \text{prefire_NDVI}} * \text{nbhd_stdev_NDVI}_i * \text{prefire_NDVI}_i +$$

$$\beta_{\text{nbhd_stdev_NDVI} * \text{nbhd_mean_NDVI}} * \text{nbhd_stdev_NDVI}_i * \text{nbhd_mean_NDVI}_i +$$

$$\beta_{\text{nbhd_mean_NDVI} * \text{prefire_NDVI}} * \text{nbhd_mean_NDVI}_i * \text{prefire_NDVI}_i +$$

$$\gamma_j$$

$$\gamma_j \sim \mathcal{N}(0, \sigma_{\text{fire}})$$

203 **Assessing the “scale of effect” of forest structure variability**

204 Each neighborhood size (90m, 150m, 210m, 270m on a side) was substituted in turn for the neighborhood
 205 standard deviation of NDVI, neighborhood mean NDVI, and terrain ruggedness covariates to generate a
 206 candidate set of 4 models. To assess the scale at which the forest structure variability effect manifests, we
 207 compared the 4 candidate models based on different neighborhood sizes using leave-one-out cross validation
 208 (LOO cross validation) (84). We inferred that the neighborhood size window used in the best-performing
 209 model reflected the scale at which the forest structure variability effect had the most support (49).

210 **Statistical software**

211 We used R for all statistical analyses (73). We used the `brms` package to fit mixed effects models in a Bayesian
 212 framework which implements the No U-Turn Sampler (NUTS) extension to the Hamiltonian Monte Carlo
 213 algorithm (85, 86). We used 4 chains with 3000 samples per chain (1500 warmup samples and 1500 posterior
 214 samples) and chain convergence was assessed for each estimated parameter by ensuring Rhat values were less
 215 than or equal to 1.01 (86).

216 Data availability

217 All data and analysis code are available via the Open Science Framework (DOI: 10.17605/OSF.IO/27NSR)
218 including a new dataset representing wildfire severity, vegetation characteristics, and regional climate conditions
219 within the perimeters of 1,090 fires from the FRAP database that burned in yellow pine/mixed-conifer forest
220 in the Sierra Nevada, California between 1984 and 2017.

221 Results

222 Programmatic assessment of severity

223 Our method to calculate remotely sensed severity using automated Landsat image fetching calibrates as well
224 or better to ground-based severity data than most other reported methods that use hand-curation of Landsat
225 imagery (see review in (87)). Further, several combinations of remotely sensed severity metrics, time windows,
226 and interpolation methods validate well with the ground-based severity metrics, including those based on
227 NDVI which is calculated using reflectance in shorter wavelengths than those typically used for measuring
228 severity (Fig. 2). The top three configurations of our remotely sensed severity metric are depicted in Fig. 2.

229 Scale of effect of forest structure variability

Tab. 1: Comparison of four models described in Eq. 2 using different neighborhood sizes for calculating forest structural variability (standard deviation of NDVI within the neighborhood), neighborhood mean NDVI, and topographic roughness. LOO is a measure of a model’s predictive accuracy (with lower values corresponding to more accurate prediction) and is calculated as -2 times the expected log pointwise predictive density (elpd) for a new dataset (84). Δ LOO is the difference between a model’s LOO and the lowest LOO in a set of models (i.e., the model with the best predictive accuracy). The Bayesian R^2 is a ‘data-based estimate of the proportion of variance explained for new data’ (88). Note that Bayesian R^2 values are conditional on the model so shouldn’t be compared across models, though they can be informative about a single model at a time.

	Neighborhood size					
	for variability	LOO	Δ LOO to	SE of Δ	LOO model	Bayesian
Model	measure	(-2*elpd)	best model	LOO	weight (%)	R^2
1	90m x 90m	40786	0	NA	100	0.299
2	150m x 150m	40842	56.03	14.69	0	0.298
3	210m x 210m	40883	96.87	20.94	0	0.297
4	270m x 270m	40912	125.9	24.73	0	0.297

230 The model with the best out-of-sample prediction accuracy assessed by leave-one-out cross validation was the
231 model fit using the smallest neighborhood size for the variability of forest structure (standard deviation of
232 neighborhood NDVI), the mean of neighborhood NDVI, and the terrain roughness (standard deviation of
233 elevation) (Tab. 1). Model weighting based on the LOO score suggests 100% of the model weight belongs to
234 the model using the smallest neighborhood size window.

235 **Effects of prefire vegetation density, 100-hour fuel moisture, potential annual** 236 **heat load, and topographic roughness on wildfire severity**

237 We report the results from fitting the model described in Eq. 2 using the smallest neighborhood size (90m
238 x 90m) because this was the best performing model (see above) and because the size and magnitude of
239 estimated coefficients were similar across neighborhood sizes (See Supp. Table 2 for a summary of all
240 parameter estimates for all models).

241 The strongest influence on the probability of a forested area burning at high-severity was the density of the
242 vegetation, as measured by the prefire NDVI at that central pixel. A greater prefire NDVI led to a greater
243 probability of high-severity fire ($\beta_{\text{prefire_ndvi}} = 1.044$; 95% CI: [0.911, 1.174]); Fig. 5). There was a strong
244 negative relationship between 100-hour fuel moisture and wildfire severity such that increasing 100-hour fuel
245 moisture was associated with a reduction in the probability of a high-severity wildfire ($\beta_{\text{fm100}} = -0.569$; 95%
246 CI: [-0.71, -0.423]) (Fig. 5). Potential annual heat load, which integrates aspect, slope, and latitude, also had
247 a strong positive relationship with the probability of a high-severity fire. Areas that were located on southwest
248 facing sloped terrain at lower latitudes had the highest potential annual heat load, and they were more likely
249 to burn at high-severity ($\beta_{\text{pahl}} = 0.239$; 95% CI: [0.208, 0.271]) Fig. 5). We found a negative effect of the
250 prefire neighborhood mean NDVI on the probability of a pixel burning at high-severity ($\beta_{\text{nbhd_mean_NDVI}} =$
251 -0.14 ; 95% CI: [-0.278, 0.002]). This is in contrast to the positive effect of the prefire NDVI of the pixel itself.
252 We found no effect of local topographic roughness on wildfire severity ($\beta_{\text{topographic_roughness}} = -0.01$; 95% CI:
253 [-0.042, 0.022]).

254 There was also a strong negative interaction between the neighborhood mean NDVI and the prefire NDVI of
255 the central pixel ($\beta_{\text{nbhd_mean_NDVI*prefire_NDVI}} = -0.573$; 95% CI: [-0.62, -0.526]).

256 **Effect of variability of vegetation structure on wildfire severity**

257 From the same model, we found strong evidence for a negative effect of variability of vegetation structure
258 on the probability of a high-severity wildfire ($\beta_{\text{nbhd_stdev_NDVI}} = -0.208$; 95% CI: [-0.247, -0.17]); Fig. 5).

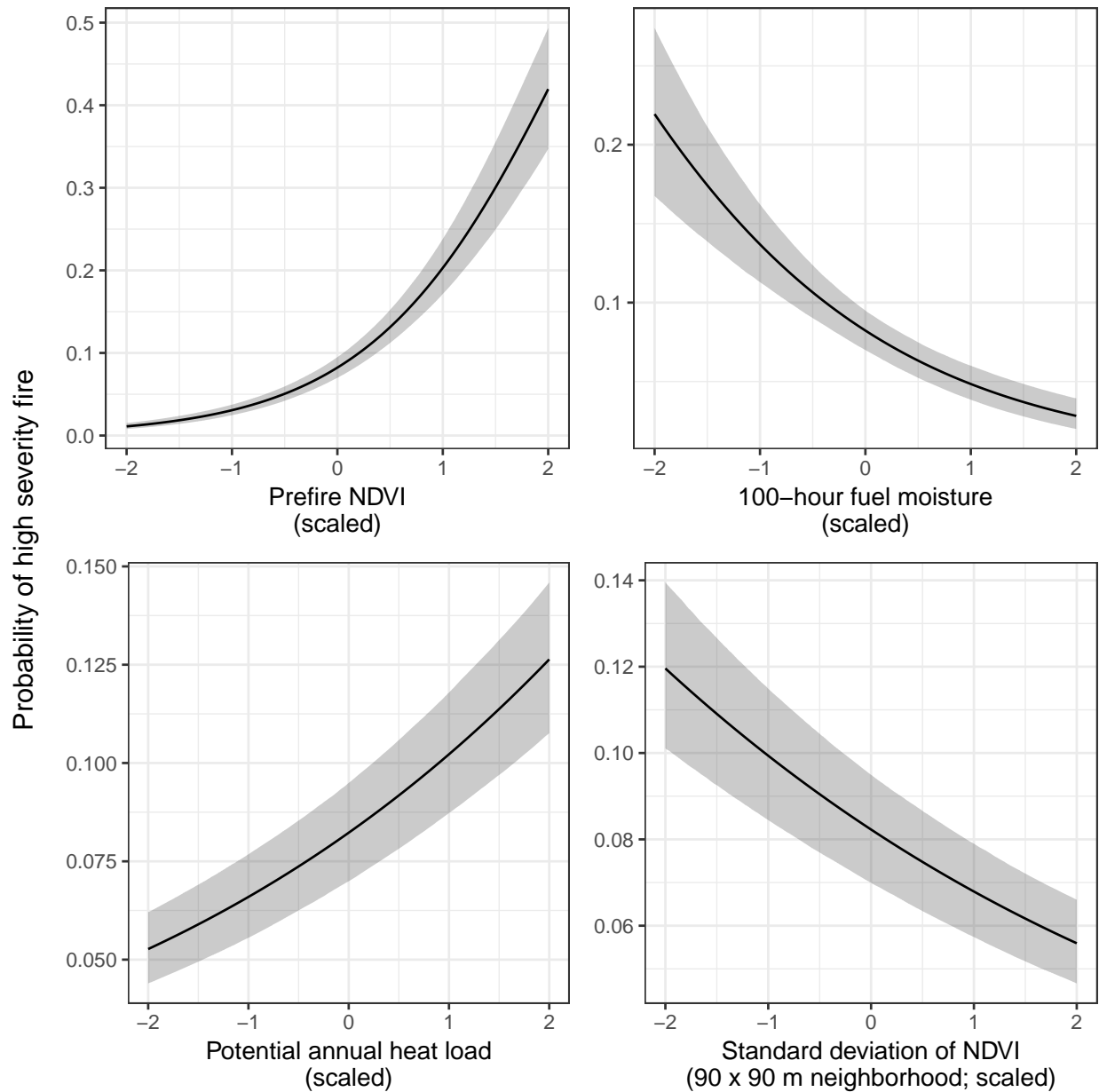


Fig. 5. The main effects and 95% credible intervals of the covariates having the strongest relationships with the probability of high-severity fire. All depicted relationships derive from the model using the 90m x 90m neighborhood size window for neighborhood standard deviation of NDVI, neighborhood mean of NDVI, and topographic roughness, as this was the best performing model of the four neighborhood sizes tested. The effect sizes of these covariates were similar for each neighborhood size tested.

259 We also found significant interactions between variability of vegetation structure and prefire NDVI of the
260 central pixel ($\beta_{\text{nbhd_stdev_NDVI*prefire_NDVI}} = 0.125$; 95% CI: [0.029, 0.218]) as well as between variability of
261 vegetation structure and neighborhood mean NDVI ($\beta_{\text{nbhd_stdev_NDVI*nbhd_mean_NDVI}} = -0.129$; 95% CI:
262 [-0.223, -0.034]).

263 Discussion

264 Broad-extent, fine-grain, spatially-explicit analyses of whole ecosystems are key to illuminating macroecological
265 phenomena such as forest resilience (89). We used a powerful, cloud-based geographic information system
266 and data repository, Google Earth Engine, as a ‘macroscope’ (90) to study feedbacks between vegetation
267 structure and wildfire disturbance in yellow pine/mixed-conifer forests of California’s Sierra Nevada mountain
268 range. With this approach, we reveal and quantify general features of this forest system, and gain deeper
269 insights into the mechanisms underlying its function.

270 High-severity wildfire in the context of ecological resilience

271 Wildfire severity can be considered a direct correlate of a forest’s resistance– the ease or difficulty with which
272 a disturbance changes the system state (8, 91). One relevant state change for assessing ecosystem resistance
273 is the loss of its characteristic native biota (92), which could be represented as overstory tree mortality (e.g.,
274 severity) in a forested system. The same fire behavior in two different forest systems (e.g., old-growth conifer
275 versus young conifer plantation) may have very different abilities to cause overstory mortality (23), which
276 reflects differences in each forest’s resistance. Resistance is a key component of resilience (8, 91) and, in this
277 framework, one manifestation of forest resilience is high resistance to wildfire, whereby some mechanism
278 leads to lower severity when a fire occurs. Here, we show clear evidence that structural heterogeneity fulfills
279 this mechanistic resistance role in dry coniferous systems (Fig. 5). This does not imply that resistance to
280 fire is the only (or a necessary) path to resilience. For instance, high-severity fire is characteristic of other
281 forest systems such as serotinous lodgepole pine forests in Yellowstone National Park, and is not ordinarily
282 expected to hamper forest regeneration (93). Our inference that structural variability is a fundamental
283 resilience mechanism in dry coniferous forests is strengthened by its large effect size and our ability to measure
284 the negative feedback phenomenon at relevant spatiotemporal scales: we captured local-scale variability in
285 structure and wildfire severity at broad spatial extents for an extensive set of nearly 1,000 fires across a
286 33-year time span.

287 **Factors influencing the probability of high-severity wildfire**

288 We found that the strongest influence on the probability of high-severity wildfire was prefire NDVI. Greater
289 NDVI corresponds to high canopy cover and vegetation density (75) which translates directly to live fuel
290 loads in the forest canopy and can increase high-severity fire (70). Overstory canopy cover and density also
291 correlate with surface fuel loads (77, 78), which play a larger role in driving high-severity fire compared to
292 canopy fuel loads in these forests (79). Thus NDVI is likely a strong predictor of fire severity because it is
293 correlated with both surface fuel loads and canopy live fuel density.

294 We found a strong positive effect of potential annual heat load as well as a strong negative effect of 100-hour
295 fuel moisture, results which corroborates similar studies (70). Some work has shown that terrain ruggedness
296 (94), and particularly coarser-scale terrain ruggedness (95), is an important predictor of wildfire severity, but
297 we found no effect using our measure of local terrain variability.

298 Critically, we found a strong negative effect of forest structural variability on wildfire severity that was
299 opposite in direction but similar in magnitude to the effect of potential annual heat load. Just as the
300 positive effect of NDVI is likely driven by surface fuel loads, the negative effect of variability in NDVI (our
301 measure of structural variability), is likely driven by discontinuity in surface fuel loads, which can reduce
302 the probability of initiation and spread of tree-killing crown fires (41, 43, 96, 97). The strong influence of
303 a decreased connectivity of fuels at a local scale suggests that heterogeneity in forest structure may also
304 influence broader-scale wildfire behavior and effects via cross-scale interactions (11, 98).

305 **Feedback between forest structural variability and wildfire severity**

306 This system-wide inverse relationship between structural variability and wildfire severity closes a feedback that
307 links past and future fire behavior via forest structure. Frequent wildfire in dry coniferous forests generates
308 variable forest structure (39, 99, 100), which in turn, as we demonstrate, dampens the severity of future fire.
309 In contrast, exclusion of wildfire homogenizes forest structure and increases the probability that a fire, when
310 it occurs, will produce large, contiguous patches of overstory mortality (24, 37). The proportion and spatial
311 configuration of fire severity in fire-prone forests are key determinants of their long-term persistence (24, 37).
312 Lower-severity fire or scattered patches of higher-severity fire reduce the risk of conversion to a non-forest
313 vegetation type (24, 101), while prospects for forest regeneration are bleak when high-severity patch sizes
314 are much larger than the natural range of variation for the system (3, 24, 26, 30, 44, 102, 103). Thus, the
315 forest-structure-mediated feedback between past and future fire severity underlies the resilience of the Sierra
316 Nevada yellow pine/mixed-conifer system.

317 **Scale of effect of variability in forest structure**

318 We found that the effect of a forest patch’s neighborhood characteristics on the probability of high-severity
319 fire was strongest at the smallest neighborhood size that we tested, 90m x 90m. This suggests that the
320 moderating effect of variability in vegetation structure on fire severity is a very local phenomenon. This
321 corroborates work by (104), who found that crown fires (with high tree killing potential) were almost always
322 reduced to surface fires (with low tree killing potential) within 70m of entering an fuel reduction treatment
323 area.

324 Severity patterns at a landscape scale (e.g., for a whole fire) may represent cross-scale emergences (89) of
325 very local interactions between forest structure and fire behavior. For instance, forest management actions
326 (e.g., prescribed fire, use of wildfire under mild conditions) that reduce fuel loads and increase structural
327 variability can be effective at reducing fire severity across broader spatial extents than the direct footprints
328 of those actions (43, 44, 105). Some work suggests that this sort of cross-scale emergence may depend on
329 even broader-scale effects of fire weather, with small-scale variability failing to influence fire behavior under
330 extreme conditions (11, 106), though we did not detect such an interaction between our metric of burning
331 conditions (100-hour fuel moisture) and variability in forest structure.

332 **Correlation between covariates and interactions**

333 Unexpectedly, we found a strong interaction between the prefire NDVI at a pixel and its neighborhood mean
334 NDVI on the probability of high-severity fire. These two variables are strongly correlated (Spearman’s $\rho =$
335 0.97), so the general effect of this interaction is to dampen the dominating effect of prefire NDVI. Thus,
336 though the marginal effect of prefire NDVI on the probability of high-severity fire is still positive and
337 large, its real-world effect might be more comparable to other modeled covariates when including the
338 negative main effect of neighborhood mean NDVI, the negative interaction effect of prefire NDVI and
339 neighborhood mean NDVI, and their tendency to covary (compare the effect of vegetation density under
340 the common scenario of prefire NDVI and neighborhood mean NDVI increasing or decreasing together:
341 $\beta_{\text{prefire_ndvi}} + \beta_{\text{nbhd_mean_NDVI}} + \beta_{\text{nbhd_mean_NDVI} * \text{prefire_NDVI}} = 0.331$, to the effect of 100-hour fuel moisture,
342 which becomes the effect with the greatest magnitude: $\beta_{\text{fm100}} = -0.569$).

343 In the few cases when prefire NDVI and the neighborhood mean NDVI contrast, there is an overall effect
344 of increasing the probability of high-severity fire. When prefire NDVI at the central pixel is high and the
345 neighborhood NDVI is low (e.g., an isolated vegetation patch; Supplemental Fig. 2), the probability of
346 high-severity fire is expected to dramatically increase. When prefire NDVI at the central pixel is low and

347 the neighborhood NDVI is high (e.g., a hole in the center of an otherwise dense forest; Supplemental Fig.
348 2), the probability of high-severity fire at that central pixel is still expected to be fairly high even though
349 there is limited vegetation density (see Supplemental Fig. 2). In these forest NDVI datasets, when these
350 variables do decouple, they tend to do so in the “hole in the forest” case and lead to a greater probability
351 of high-severity fire at the central pixel despite the lower vegetation density there. This can perhaps be
352 explained if the consistently high vegetation density in a local neighborhood— itself more likely to burn at
353 high-severity— exerts a contagious effect on the central pixel, raising its probability of burning at high-severity
354 regardless of how much fuel might be there to burn.

355 **A new approach to remotely sensing wildfire severity**

356 We developed an approach to calculating wildfire severity leveraging the cloud-based data catalog, the large
357 parallel processing system, and the distribution of computation tasks in Google Earth Engine to enable
358 rapid high-throughput analyses of earth observation data (52). Our programmatic assessment of wildfire
359 severity across the 972 Sierra Nevada yellow pine/mixed-conifer fires in the FRAP perimeter database, which
360 enabled consistent assessment of severity for a broad representation of fires including smaller events (60). We
361 found that the relative burn ratio (RBR) calculated using prefire Landsat images collected over a 48-day
362 period prior to the fire and postfire Landsat images collected over a 48-day period one year after the prefire
363 images validated the best with ground-based severity measurements (composite burn index; CBI). Further,
364 we found that this programmatic approach was robust to a wide range of severity metrics, time windows, and
365 interpolation techniques.

366 We echo the conclusion of (63) that the validation of differences between pre- and postfire NDVI to field-
367 measured severity data, which uses near infrared reflectance, is comparable to validation using more commonly
368 used severity metrics (e.g., RdNBR and RBR) that rely on short wave infrared reflectance. One immediately
369 operational implication of this is that the increasing availability of low-cost small unhumanned aerial systems
370 (sUAS a.k.a. drones) and near-infrared-detecting imagers (e.g., those used for agriculture monitoring) may be
371 used to reliably assess wildfire severity at very high spatial resolutions.

372 **Conclusions**

373 While the severity of a wildfire in any given place is controlled by many variables, we have presented strong
374 evidence that, across large areas of forest, variable forest structure generally makes yellow pine/mixed-conifer
375 forest in the Sierra Nevada more resistant to this inevitable disturbance. It has been well-documented that
376 frequent, low-severity wildfire maintains forest structural variability. Here, we demonstrate a system-wide

377 reciprocal effect suggesting that greater local-scale variability of vegetation structure makes fire-prone, dry
378 forests more resilient to wildfire and may increase the probability of their long-term persistence.

379 **Acknowledgements**

380 We thank Connie Millar, Derek Young, and Meagan Oldfather for valuable comments about this work and
381 we also thank the community of Google Earth Engine developers for prompt and helpful insights about the
382 platform. We thank two anonymous reviewers for their helpful comments on the manuscript. Funding was
383 provided by NSF Graduate Research Fellowship Grant #DGE- 1321845 Amend. 3 (to MJK).

384 **References**

- 385 1. Hansen MC, et al. (2013) High-Resolution Global Maps of 21st-Century Forest Cover Change. *Science*
386 342(6160):850–853.
- 387 2. Crowther TW, et al. (2015) Mapping tree density at a global scale. *Nature* 525(7568):201–205.
- 388 3. Millar CI, Stephenson NL (2015) Temperate forest health in an era of emerging megadisturbance. *Science*
389 349(6250):823–826.
- 390 4. Trumbore S, Brando P, Hartmann H (2015) Forest health and global change. *Science* 349(6250):814–818.
- 391 5. Seidl R, Spies TA, Peterson DL, Stephens SL, Hicke JA (2016) Searching for resilience: Addressing the
392 impacts of changing disturbance regimes on forest ecosystem services. *J Appl Ecol* 53(1):120–129.
- 393 6. Schoennagel T, et al. (2017) Adapt to more wildfire in western North American forests as climate changes.
394 *Proceedings of the National Academy of Sciences* 114(18):4582–4590.
- 395 7. Holling CS (1973) Resilience and Stability of Ecological Systems. *Annual Review of Ecology and*
396 *Systematics*:1–23.
- 397 8. Walker B, Holling CS, Carpenter SR, Kinzig AP (2004) Resilience, Adaptability and Transformability in
398 Social-ecological Systems. *Ecology and Society* 9(2). doi:10.5751/ES-00650-090205.
- 399 9. Scheffer M (2009) *Critical Transitions in Nature and Society* (Princeton University Press).
- 400 10. Reyer CPO, et al. (2015) Forest resilience and tipping points at different spatio-temporal scales:
401 Approaches and challenges. *Journal of Ecology* 103(1):5–15.
- 402 11. Peters DPC, et al. (2004) Cross-scale interactions, nonlinearities, and forecasting catastrophic events.

- 403 *Proceedings of the National Academy of Sciences* 101(42):15130–15135.
- 404 12. Reusch TBH, Ehlers A, Hammerli A, Worm B (2005) Ecosystem recovery after climatic extremes enhanced
405 by genotypic diversity. *Proceedings of the National Academy of Sciences* 102(8):2826–2831.
- 406 13. Baskett ML, Gaines SD, Nisbet RM (2009) Symbiont diversity may help coral reefs survive moderate
407 climate change. *Ecological Applications* 19(1):3–17.
- 408 14. Agashe D (2009) The Stabilizing Effect of Intraspecific Genetic Variation on Population Dynamics in
409 Novel and Ancestral Habitats. *The American Naturalist* 174(2):255–267.
- 410 15. Tilman D (1994) Competition and Biodiversity in Spatially Structured Habitats. *Ecology* 75(1):2–16.
- 411 16. Chesson P (2000) Mechanisms of Maintenance of Species Diversity. *Annual Review of Ecology and*
412 *Systematics* 31(1):343–366.
- 413 17. Cadotte M, Albert CH, Walker SC (2013) The ecology of differences: Assessing community assembly
414 with trait and evolutionary distances. *Ecology Letters* 16(10):1234–1244.
- 415 18. Gazol A, Camarero JJ (2016) Functional diversity enhances silver fir growth resilience to an extreme
416 drought. *Journal of Ecology* 104(4):1063–1075.
- 417 19. Ackerly DD, et al. (2010) The geography of climate change: Implications for conservation biogeography:
418 Geography of climate change. *Diversity and Distributions* 16(3):476–487.
- 419 20. Lenoir J, et al. (2013) Local temperatures inferred from plant communities suggest strong spatial buffering
420 of climate warming across Northern Europe. *Global Change Biology* 19(5):1470–1481.
- 421 21. Questad EJ, Foster BL (2008) Coexistence through spatio-temporal heterogeneity and species sorting in
422 grassland plant communities. *Ecology Letters* 11(7):717–726.
- 423 22. Reyser CP, Rammig A, Brouwers N, Langerwisch F (2015) Forest resilience, tipping points and global
424 change processes. *Journal of Ecology* 103(1):1–4.
- 425 23. Keeley JE (2009) Fire intensity, fire severity and burn severity: A brief review and suggested usage.
426 *International Journal of Wildland Fire* 18(1):116.
- 427 24. Stevens JT, Collins BM, Miller JD, North MP, Stephens SL (2017) Changing spatial patterns of
428 stand-replacing fire in California conifer forests. *Forest Ecology and Management* 406:28–36.
- 429 25. Davis KT, et al. (2019) Wildfires and climate change push low-elevation forests across a critical climate

- 430 threshold for tree regeneration. *PNAS*:201815107.
- 431 26. Safford HD, Stevens JT (2017) *Natural Range of Variation for Yellow Pine and Mixed-Conifer Forests in*
432 *the Sierra Nevada, Southern Cascades, and Modoc and Inyo National Forests, California, USA.*
- 433 27. Welch KR, Safford HD, Young TP (2016) Predicting conifer establishment post wildfire in mixed conifer
434 forests of the North American Mediterranean-climate zone. *Ecosphere* 7(12):e01609.
- 435 28. Young DJN, et al. (2019) Post-fire forest regeneration shows limited climate tracking and potential for
436 drought-induced type conversion. *Ecology* 100(2):e02571.
- 437 29. Collins BM, Roller GB (2013) Early forest dynamics in stand-replacing fire patches in the northern Sierra
438 Nevada, California, USA. *Landscape Ecology* 28(9):1801–1813.
- 439 30. Coppoletta M, Merriam KE, Collins BM (2016) Post-fire vegetation and fuel development influences fire
440 severity patterns in reburns. *Ecological Applications* 26(3):686–699.
- 441 31. Williams AP, et al. (2013) Temperature as a potent driver of regional forest drought stress and tree
442 mortality. *Nature Climate Change* 3(3):292–297.
- 443 32. Clark JS, et al. (2016) The impacts of increasing drought on forest dynamics, structure, and biodiversity
444 in the United States. *Global Change Biology* 22(7):2329–2352.
- 445 33. Fried JS, Torn MS, Mills E (2004) The Impact of Climate Change on Wildfire Severity: A Regional
446 Forecast for Northern California. *Climatic Change* 64(1/2):169–191.
- 447 34. Abatzoglou JT, Williams AP (2016) Impact of anthropogenic climate change on wildfire across western
448 US forests. *Proceedings of the National Academy of Sciences* 113(42):11770–11775.
- 449 35. Stevens-Rumann CS, et al. (2018) Evidence for declining forest resilience to wildfires under climate
450 change. *Ecology Letters* 21(2):243–252.
- 451 36. Miller JD, Thode AE (2007) Quantifying burn severity in a heterogeneous landscape with a relative
452 version of the delta Normalized Burn Ratio (dNBR). *Remote Sensing of Environment* 109(1):66–80.
- 453 37. Steel ZL, Koontz MJ, Safford HD (2018) The changing landscape of wildfire: Burn pattern trends and
454 implications for California’s yellow pine and mixed conifer forests. *Landscape Ecology* 33(7):1159–1176.
- 455 38. Stephens SL, Fry DL, Franco-Vizcaíno E (2008) Wildfire and Spatial Patterns in Forests in Northwestern
456 Mexico: The United States Wishes It Had Similar Fire Problems. *Ecology and Society* 13(2). doi:10.5751/ES-

457 02380-130210.

458 39. North M, Stine P, O'Hara K, Zielinski W, Stephens S (2009) *An ecosystem management strategy for*
459 *Sierran mixed-conifer forests* (U.S. Department of Agriculture, Forest Service, Pacific Southwest Research
460 Station, Albany, CA) doi:10.2737/PSW-GTR-220.

461 40. Virah-Sawmy M, Gillson L, Willis KJ (2009) How does spatial heterogeneity influence resilience to
462 climatic changes? Ecological dynamics in southeast Madagascar. *Ecological Monographs* 79(4):557–574.

463 41. Agee JK (1996) The influence of forest structure on fire behavior. *17th Forest Vegetation Management*
464 *Conference*:17.

465 42. Scott JH, Reinhardt ED (2001) *Assessing crown fire potential by linking models of surface and crown fire*
466 *behavior* (U.S. Department of Agriculture, Forest Service, Rocky Mountain Research Station, Ft. Collins,
467 CO) doi:10.2737/RMRS-RP-29.

468 43. Graham RT, McCaffrey S, Jain TB (2004) *Science basis for changing forest structure to modify wildfire*
469 *behavior and severity* (U.S. Department of Agriculture, Forest Service, Rocky Mountain Research Station, Ft.
470 Collins, CO) doi:10.2737/RMRS-GTR-120.

471 44. Stephens SL, et al. (2009) Fire treatment effects on vegetation structure, fuels, and potential fire severity
472 in western U.S. forests. *Ecological Applications* 19(2):305–320.

473 45. Fox JM, Whitesides GM (2015) Warning signals for eruptive events in spreading fires. *Proceedings of the*
474 *National Academy of Sciences* 112(8):2378–2383.

475 46. Sugihara NG, Wagtendonk JWV, Fites-Kaufman J, Shaffer KE, Thode AE (2006) *Fire in California's*
476 *ecosystems* (University of California Press) Available at: [https://nau.pure.elsevier.com/en/publications/](https://nau.pure.elsevier.com/en/publications/fire-in-californias-ecosystems)
477 [fire-in-californias-ecosystems](https://nau.pure.elsevier.com/en/publications/fire-in-californias-ecosystems) [Accessed April 23, 2019].

478 47. Scholl AE, Taylor AH (2010) Fire regimes, forest change, and self-organization in an old-growth
479 mixed-conifer forest, Yosemite National Park, USA. *Ecological Applications* 20(2):362–380.

480 48. Moritz MA, Morais ME, Summerell LA, Carlson JM, Doyle J (2005) Wildfires, complexity, and highly
481 optimized tolerance. *Proceedings of the National Academy of Sciences* 102(50):17912–17917.

482 49. Graham LJ, Spake R, Gillings S, Watts K, Eigenbrod F (2019) Incorporating fine-scale environmental
483 heterogeneity into broad-extent models. *Methods in Ecology and Evolution* 10(6):767–778.

484 50. Kotliar NB, Wiens JA (1990) Multiple Scales of Patchiness and Patch Structure: A Hierarchical Framework

- 485 for the Study of Heterogeneity. *Oikos* 59(2):253.
- 486 51. Turner MG, Donato DC, Romme WH (2013) Consequences of spatial heterogeneity for ecosystem services
487 in changing forest landscapes: Priorities for future research. *Landscape Ecology* 28(6):1081–1097.
- 488 52. Gorelick N, et al. (2017) Google Earth Engine: Planetary-scale geospatial analysis for everyone. *Remote*
489 *Sensing of Environment* 202:18–27.
- 490 53. Haralick RM, Shanmugam K, Dinstein I (1973) Textural Features for Image Classification. *IEEE*
491 *Transactions on Systems, Man, and Cybernetics* SMC-3(6):610–621.
- 492 54. JepsonFloraProject ed. (2016) *Jepson eFlora* Available at: <http://ucjeps.berkeley.edu/eflora/> [Accessed
493 March 7, 2016].
- 494 55. Eidenshink J, et al. (2007) A Project for Monitoring Trends in Burn Severity. *Fire Ecology* 3(1):3–21.
- 495 56. Masek J, et al. (2006) A Landsat Surface Reflectance Dataset for North America, 19902000. *IEEE*
496 *Geoscience and Remote Sensing Letters* 3(1):68–72.
- 497 57. Vermote E, Justice C, Claverie M, Franch B (2016) Preliminary analysis of the performance of the
498 Landsat 8/OLI land surface reflectance product. *Remote Sensing of Environment* 185:46–56.
- 499 58. USGS (2017) Landsat 8 Surface Reflectance Code (LASRC) Product Guide. 40.
- 500 59. USGS (2017) Landsat 4-7 Surface Reflectance (LEDAPS) Product Guide. 41.
- 501 60. Randerson JT, Chen Y, Werf GR van der, Rogers BM, Morton DC (2012) Global burned area and
502 biomass burning emissions from small fires. *Journal of Geophysical Research: Biogeosciences* 117(G4).
503 doi:10.1029/2012JG002128.
- 504 61. Miller JD, Skinner CN, Safford HD, Knapp EE, Ramirez CM (2012) Trends and causes of severity, size,
505 and number of fires in northwestern California, USA. *Ecological Applications* 22(1):184–203.
- 506 62. Miller JD, Safford H (2012) TRENDS IN WILDFIRE SEVERITY: 1984 TO2010 IN THE SIERRA
507 NEVADA, MODOC PLATEAU, AND SOUTHERN CASCADES, CALIFORNIA, USA. *Fire Ecology* 8(3):41–
508 57.
- 509 63. Zhu Z, Key C, Ohlen D, Benson N (2006) *Evaluate Sensitivities of Burn-Severity Mapping Algorithms*
510 *for Different Ecosystems and Fire Histories in the United States*.
- 511 64. Sikkink PG, et al. (2013) Composite Burn Index (CBI) data and field photos collected for the FIRESEV

- 512 project, western United States. doi:10.2737/RDS-2013-0017.
- 513 65. Key CH, Benson NC (2006) Landscape Assessment (LA). 55.
- 514 66. Miller JD, et al. (2009) Calibration and validation of the relative differenced Normalized Burn Ratio
515 (RdNBR) to three measures of fire severity in the Sierra Nevada and Klamath Mountains, California, USA.
516 *Remote Sensing of Environment* 113(3):645–656.
- 517 67. Cansler CA, McKenzie D (2012) How Robust Are Burn Severity Indices When Applied in a New Region?
518 Evaluation of Alternate Field-Based and Remote-Sensing Methods. *Remote Sensing* 4(2):456–483.
- 519 68. Parks S, Dillon G, Miller C (2014) A New Metric for Quantifying Burn Severity: The Relativized Burn
520 Ratio. *Remote Sensing* 6(3):1827–1844.
- 521 69. Prichard SJ, Kennedy MC (2014) Fuel treatments and landform modify landscape patterns of burn
522 severity in an extreme fire event. *Ecological Applications* 24(3):571–590.
- 523 70. Parks SA, et al. (2018) High-severity fire: Evaluating its key drivers and mapping its probability across
524 western US forests. *Environmental Research Letters* 13(4):044037.
- 525 71. Wickham H (2019) *Modelr: Modelling Functions that Work with the Pipe* Available at: [https://CRAN.](https://CRAN.R-project.org/package=modelr)
526 [R-project.org/package=modelr](https://CRAN.R-project.org/package=modelr).
- 527 72. Henry L, Wickham H (2019) *Purrr: Functional Programming Tools* Available at: [https://CRAN.R-project.](https://CRAN.R-project.org/package=purrr)
528 [org/package=purrr](https://CRAN.R-project.org/package=purrr).
- 529 73. R Core Team (2018) *R: A Language and Environment for Statistical Computing* (R Foundation for
530 Statistical Computing, Vienna, Austria) Available at: <https://www.R-project.org/>.
- 531 74. Tuanmu M-N, Jetz W (2015) A global, remote sensing-based characterization of terrestrial habitat
532 heterogeneity for biodiversity and ecosystem modelling: Global habitat heterogeneity. *Global Ecology and*
533 *Biogeography* 24(11):1329–1339.
- 534 75. Rouse W, Haas RH, Deering W, Schell JA (1973) *MONITORING THE VERNAL ADVANCEMENT*
535 *AND RETROGRADATION (GREEN WAVE EFFECT) OF NATURAL VEGETATION* (Goddard Space
536 Flight Center, Greenbelt, MD, USA).
- 537 76. Franklin J, Logan T, Woodcock C, Strahler A (1986) Coniferous Forest Classification and Inventory Using
538 Landsat and Digital Terrain Data. *IEEE Transactions on Geoscience and Remote Sensing* GE-24(1):139–149.
- 539 77. Lydersen JM, Collins BM, Knapp EE, Roller GB, Stephens S (2015) Relating fuel loads to overstorey
540 structure and composition in a fire-excluded Sierra Nevada mixed conifer forest. *International Journal of*

- 541 *Wildland Fire* 24(4):484.
- 542 78. Collins BM, et al. (2016) Variability in vegetation and surface fuels across mixed-conifer-dominated
543 landscapes with over 40 years of natural fire. *Forest Ecology and Management* 381:74–83.
- 544 79. Stephens SL, et al. (2012) The Effects of Forest Fuel-Reduction Treatments in the United States.
545 *BioScience* 62(6):549–560.
- 546 80. Farr TG, et al. (2007) The Shuttle Radar Topography Mission. *Reviews of Geophysics* 45(2).
547 doi:10.1029/2005RG000183.
- 548 81. McCune B, Keon D (2002) Equations for potential annual direct incident radiation and heat load. *Journal*
549 *of Vegetation Science* 13(4):603–606.
- 550 82. McCune B (2007) Improved estimates of incident radiation and heat load using non- parametric regression
551 against topographic variables. *Journal of Vegetation Science* 18(5):751–754.
- 552 83. Abatzoglou JT (2013) Development of gridded surface meteorological data for ecological applications and
553 modelling. *International Journal of Climatology* 33(1):121–131.
- 554 84. Vehtari A, Gelman A, Gabry J (2017) Practical Bayesian model evaluation using leave-one-out cross-
555 validation and WAIC. *Statistics and Computing* 27(5):1413–1432.
- 556 85. Hoffman MD, Gelman A (2014) The No-U-Turn Sampler: Adaptively Setting Path Lengths in Hamiltonian
557 Monte Carlo. *Journal of Machine Learning Research* 15:31.
- 558 86. Bürkner P-C (2017) **Brms** : An R Package for Bayesian Multilevel Models Using Stan. *Journal of*
559 *Statistical Software* 80(1). doi:10.18637/jss.v080.i01.
- 560 87. Edwards AC, Russell-Smith J, Maier SW (2018) A comparison and validation of satellite-derived fire
561 severity mapping techniques in fire prone north Australian savannas: Extreme fires and tree stem mortality.
562 *Remote Sensing of Environment* 206:287–299.
- 563 88. Gelman A, Goodrich B, Gabry J, Vehtari A (2018) R-squared for Bayesian regression models. *The*
564 *American Statistician*:1–6.
- 565 89. Heffernan JB, et al. (2014) Macrosystems ecology: Understanding ecological patterns and processes at
566 continental scales. *Frontiers in Ecology and the Environment* 12(1):5–14.
- 567 90. Beck J, et al. (2012) What’s on the horizon for macroecology? *Ecography* 35(8):673–683.
- 568 91. Folke C, et al. (2004) Regime Shifts, Resilience, and Biodiversity in Ecosystem Management. *Annual*

- 569 *Review of Ecology, Evolution, and Systematics* 3:557–581.
- 570 92. Keith DA, et al. (2013) Scientific Foundations for an IUCN Red List of Ecosystems. *PLoS ONE*
571 8(5):e62111.
- 572 93. Turner MG, Romme WH, Gardner RH, Hargrove WW (1997) Effects of Fire Size and Pattern on Early
573 Succession in Yellowstone National Park. *Ecological Monographs* 67(4):411.
- 574 94. Holden ZA, Morgan P, Evans JS (2009) A predictive model of burn severity based on 20-year satellite-
575 inferred burn severity data in a large southwestern US wilderness area. *Forest Ecology and Management*
576 258(11):2399–2406.
- 577 95. Dillon GK, et al. (2011) Both topography and climate affected forest and woodland burn severity in two
578 regions of the western US, 1984 to 2006. *Ecosphere* 2(12):art130.
- 579 96. Wagner CEV (1977) Conditions for the start and spread of crown fire. *Can J For Res* 7(1):23–34.
- 580 97. Agee JK, Skinner CN (2005) Basic principles of forest fuel reduction treatments. *Forest Ecology and*
581 *Management* 211(1-2):83–96.
- 582 98. Rose KC, et al. (2017) Historical foundations and future directions in macrosystems ecology. *Ecology*
583 *Letters* 20(2):147–157.
- 584 99. Larson AJ, Churchill D (2012) Tree spatial patterns in fire-frequent forests of western North America,
585 including mechanisms of pattern formation and implications for designing fuel reduction and restoration
586 treatments. *Forest Ecology and Management* 267:74–92.
- 587 100. Malone S, et al. (2018) Mixed-Severity Fire Fosters Heterogeneous Spatial Patterns of Conifer
588 Regeneration in a Dry Conifer Forest. *Forests* 9(1):45.
- 589 101. Walker RB, Coop JD, Parks SA, Trader L (2018) Fire regimes approaching historic norms reduce
590 wildfire-facilitated conversion from forest to non-forest. *Ecosphere* 9(4):e02182.
- 591 102. Wagtendonk JWV (2006) *Fire as a Physical Process* (University of California Press) Available
592 at: [http://california.universitypressscholarship.com/view/10.1525/california/9780520246058.001.0001/
593 upso-9780520246058-chapter-3](http://california.universitypressscholarship.com/view/10.1525/california/9780520246058.001.0001/upso-9780520246058-chapter-3) [Accessed April 23, 2019].
- 594 103. Miller JD, Safford HD (2017) Corroborating Evidence of a Pre-Euro-American Low- to Moderate-
595 Severity Fire Regime in Yellow Pine Mixed Conifer Forests of the Sierra Nevada, California, USA. *Fire Ecology*
596 13(1):58–90.
- 597 104. Safford H, Stevens J, Merriam K, Meyer M, Latimer A (2012) Fuel treatment effectiveness in California

598 yellow pine and mixed conifer forests. *Forest Ecology and Management* 274:17–28.

599 105. Tubbesing CL, et al. (2019) Strategically placed landscape fuel treatments decrease fire severity and
600 promote recovery in the northern Sierra Nevada. *Forest Ecology and Management* 436:45–55.

601 106. Lydersen JM, North MP, Collins BM (2014) Severity of an uncharacteristically large wildfire, the Rim
602 Fire, in forests with relatively restored frequent fire regimes. *Forest Ecology and Management* 328:326–334.